

# Natural orbital description of the halo nucleus ${}^6\text{He}$

Chrysovalantis Constantinou\* and Mark A. Caprio

*Department of Physics, University of Notre Dame, Notre Dame, Indiana 46556-5670, USA*

James P. Vary and Pieter Maris

*Department of Physics and Astronomy, Iowa State University, Ames, Iowa 50011-3160, USA*

(Dated: February 7, 2018)

*Ab initio* calculations of nuclei face the challenge of simultaneously describing strong short-range internucleon correlations and the long-range properties of weakly-bound halo nucleons. Natural orbitals, which diagonalize the one-body density matrix, provide a basis which is better matched to the physical structure of the many-body wave function. We demonstrate that the use of natural orbitals significantly improves convergence for *ab initio* no-core configuration interaction calculations of the neutron halo nucleus  ${}^6\text{He}$ , relative to the traditional oscillator basis.

PACS numbers: 21.60.Cs, 21.10.-k, 27.20.+n

## I. INTRODUCTION

*Ab initio* calculations of nuclear structure [1–9] face the challenge of describing a complex, multiscale quantum many-body system. The goal is to directly solve the many-body problem for a system of protons and neutrons, with realistic internucleon interactions [10–13]. However, the nucleus is governed by a strong, short-range interaction. Short-range correlations, tightly-bound  $\alpha$  clusters [14], and weakly-bound halo nucleons [15, 16] introduce dynamics over differing length scales and energy scales, within the same nucleus, which must be simultaneously described within the same many-body calculation.

Natural orbitals [17–22] provide a means of adapting the single-particle basis to better match the physical structure of the many-body wave function. Natural orbitals are obtained by diagonalizing the one-body density matrix, deduced from a preliminary many-body calculation using an initial reference single-particle basis. The Laguerre function basis [23, 24] has been used as the starting point for natural orbitals in atomic electron-structure calculations [18], while we start from the harmonic oscillator orbitals [25] more familiar to the nuclear structure context [26]. The natural orbital basis builds in important contributions from high-lying orbitals of the initial basis — for the present application, high-lying oscillator shells — thereby accelerating the convergence of wave functions, energies, and other observables.

In this work, we present a framework for *ab initio* no-core configuration interaction (NCCI) [8] calculations with a natural orbital basis and demonstrate improved convergence for the lightest neutron halo nucleus  ${}^6\text{He}$  [15]. When used with recently-proposed infrared (IR) basis-extrapolation schemes [27, 28], we show

that natural orbitals provide improved independence of basis parameters for predictions of energy and radius observables.

## II. NATURAL ORBITALS

In NCCI calculations, the nuclear many-body Schrödinger equation is formulated as a matrix eigenproblem, where the Hamiltonian is represented within a basis of Slater determinants, *i.e.*, antisymmetrized products of single-particle states. Conventionally, harmonic oscillator orbitals [25] are used, and the basis is truncated to a maximum allowed number  $N_{\text{max}}$  of oscillator excitations [8]. The calculated wave functions, energies, and observables depend upon both the truncation  $N_{\text{max}}$  and the oscillator length  $b$  of the basis (or, equivalently, the oscillator energy  $\hbar\omega \propto b^{-2}$ ). The solution of the full, untruncated many-body problem could, in principle, be obtained to any desired accuracy, by retaining a sufficiently complete basis set. However, the dimension of the NCCI problem increases rapidly with the number of nucleons and included single-particle excitations, as shown in Fig. 1. Currently available computational resources therefore limit the convergence of calculated states and observables [29–31].

We therefore seek a physically-adapted basis, in which the nuclear many-body wave function can be efficiently and accurately described, subject to the constraint of accessible problem dimensions. The *natural orbital* basis minimizes the mean occupation of states above the Fermi surface [21, 32], thus reducing the contribution of high-lying orbitals in describing the many-body wave function. Intuitively, the natural orbitals may be understood as representing an attempt to recover the basis in which the many-body wave function most resembles a single Slater determinant. Although we cannot expect to reduce the complex, highly-correlated nuclear wave function to a single Slater determinant, as assumed in the Hartree-Fock approximation, we may expect that transforming to a more natural single-particle basis could enhance the role

---

\*Present address: Center for Theoretical Physics, Sloane Physics Laboratory, Yale University, New Haven, Connecticut 06520-8120, USA.

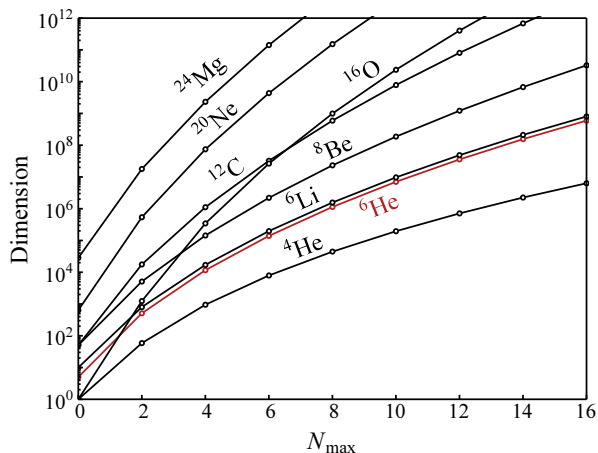


FIG. 1: Growth of the NCCI problem dimension as a function of the number of oscillator excitations  $N_{\max}$  included in the basis, for selected nuclides, including  ${}^6\text{He}$  (red curve). The dimensions shown are for spaces with zero angular momentum projection ( $M = 0$ ) and positive parity.

of a comparatively small set of dominant Slater determinants, and thereby accelerate convergence within a Slater determinant expansion.

An NCCI state of good total angular momentum can only, in general, be obtained as a superposition of several Slater determinants of  $nljm$  single particle states (here,  $n$  is the radial quantum number,  $l$  labels the orbital angular momentum,  $j$  labels the resultant angular momentum after coupling to the spin, and  $m$  labels its projection). Therefore, we cannot, in general, expect the nuclear eigenfunctions to resemble a single Slater determinant. Rather, we hope to recover wave functions which most resemble a single *configuration* of nucleons over  $nlj$  orbitals. For this purpose, we consider the *scalar densities*  $\rho_{ab}^{(0)} \equiv \langle \Psi | [c_b^\dagger \tilde{c}_a]_{00} | \Psi \rangle$ , where  $c_a^\dagger$  represents the creation operator for a nucleon in orbital  $a = (n_a l_a j_a)$  and the brackets  $[\dots]_{00}$  represent spherical tensor coupling to zero angular momentum. For a single configuration  $|\Psi\rangle$ , the scalar densities are diagonal, and the diagonal entries give the occupations of the contributing orbitals  $[\langle \mathcal{N}_a \rangle = (2j_a + 1)^{1/2} \rho_{aa}^{(0)}]$ .<sup>1</sup> Otherwise, for the general case of a many-body state  $|\Psi\rangle$ , natural orbitals are defined by diagonalizing this scalar density matrix. The scalar density matrix only connects orbitals of the same  $l$  and  $j$ , *i.e.*, differing at most in their radial quantum number  $n$ , so the transformation to natural orbitals induces a change of basis on the radial functions separately within each  $lj$  space  $[\langle n'lj \rangle = \sum_n a_{n',n}^{(lj)} |nlj\rangle]$ .

An initial NCCI calculation is carried out in the oscil-

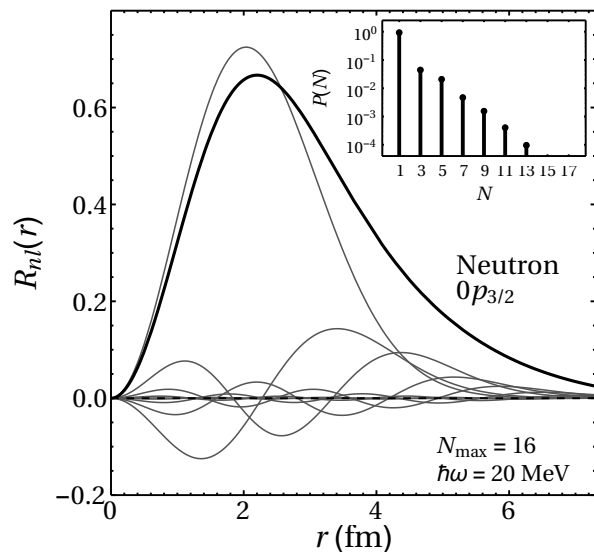


FIG. 2: Radial wave function for the neutron  $0p_{3/2}$  natural orbital (heavy curve) derived from the  ${}^6\text{He}$  ground state calculation in the harmonic oscillator basis, along with the contributions from individual oscillator basis functions (gray curves). The squared amplitudes  $P(N)$  of these contributions are shown in the inset. The initial oscillator basis for this calculation has  $N_{\max} = 16$  and  $\hbar\omega = 20$  MeV.

lator basis. This provides a scalar density matrix for the ground-state wave function, which is then diagonalized to yield the natural orbitals. The eigenvalue associated with a natural orbital represents its mean occupation in the many-body wave function. We order the natural orbitals by decreasing eigenvalue of the density matrix [21], *i.e.*, starting with  $n = 0$  for the natural orbital with highest eigenvalue  $[\langle \mathcal{N}_{0lj} \rangle \geq \langle \mathcal{N}_{1lj} \rangle \geq \dots]$ , thereby providing an  $n$  quantum number for an  $N_{\max}$ -type truncation scheme (see Ref. [33]).

The lowest  $p_{3/2}$  natural orbital obtained from the  ${}^6\text{He}$  ground-state one-body densities is illustrated in Fig. 2, taking an example from the NCCI calculations presented below. In a traditional shell-model description,  ${}^6\text{He}$  consists of two protons and two neutrons in a filled  $s$  shell ( $N \equiv 2n + l = 0$ ), plus two neutrons in the valence  $p$  shell ( $N = 1$ ). In the oscillator-basis NCCI calculations, this general structure is reflected in a nearly-filled  $s$  shell. The next most heavily occupied orbital is then the neutron  $0p_{3/2}$ . We observe that the corresponding natural orbital [Fig. 2] receives extended contributions from high-lying oscillator shells and thus acquires a substantial large- $r$  tail compared to the oscillator orbital, as may be expected for a weakly-bound halo nucleon.

The NCCI calculation using the natural orbital basis is no more computationally difficult than the original oscillator basis calculation. It is simply necessary, in preparation, to carry out a similarity transformation of the input Hamiltonian, as described in Refs. [33–35].

<sup>1</sup> That is, the total occupation number operator for an orbital is  $\mathcal{N}_a \equiv \sum_{m_a} c_{a,m_a}^\dagger c_{a,m_a} = \pm (2j_a + 1)^{1/2} [c_a^\dagger \tilde{c}_a]_{00}$ , where the sign is to be taken according to the choice of conjugation phase convention  $\tilde{c}_{a,m_a} \equiv (-)^{j_a \pm m_a} c_{a,-m_a}$ .

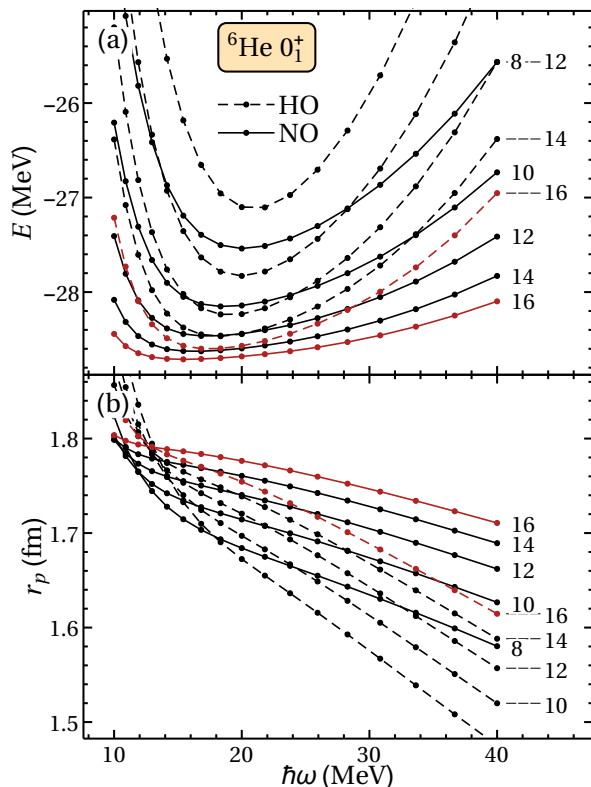


FIG. 3: Comparison of  ${}^6\text{He}$  ground state properties calculated using harmonic oscillator (HO, dashed lines) and natural orbital (NO, solid lines) bases: (a) energy and (b) ground state proton radii. These are shown as functions of the oscillator basis  $\hbar\omega$ , for  $N_{\text{max}} = 10$  to 16 (as labeled).

### III. RESULTS

Several experimental properties of the ground state of  ${}^6\text{He}$  support the interpretation that it consists of a weakly-bound two-neutron halo surrounding a tightly-bound  $\alpha$  core [15, 16]. The two-neutron separation energy for  ${}^6\text{He}$  is only 0.97 MeV, out of a total binding energy of 29.27 MeV [36]. Experimentally, the onset of halo structure along the He isotopic chain is indicated by a jump in the measured charge and matter radii, from  ${}^4\text{He}$  to  ${}^6\text{He}$ . The root mean square (RMS) point-proton distribution radius  $r_p$ , which may be deduced [37] from the measured charge radius, increases by  $\sim 32\%$  from  ${}^4\text{He}$  [ $r_p = 1.462(6)$  fm] to  ${}^6\text{He}$  [ $r_p = 1.934(9)$  fm] [38–40]. This increase may be understood as a consequence of halo structure, arising from the recoil of the charged  $\alpha$  core against the halo neutrons (as well as possible contributions from swelling of the  $\alpha$  core [40]).

The initial oscillator basis NCCI calculations from which we derive natural orbitals for  ${}^6\text{He}$  cover a range of oscillator basis parameters  $\hbar\omega = 10$  MeV to 40 MeV with truncations  $N_{\text{max}} \leq 16$ , as considered in Ref. [35]. The NCCI calculations are carried out using the code MFDn [41, 42], with the JISP16 two-body internucleon interaction [12] plus Coulomb interaction.

The ground state energy eigenvalues obtained for  ${}^6\text{He}$  using the harmonic oscillator (dashed lines) and natural orbital (solid lines) bases are compared in Fig. 3(a). The energies from the natural orbital calculations are lower (thus, by the variational principle, closer to the true value) than those from the harmonic oscillator calculations and are also less dependent upon  $\hbar\omega$ . The improvement in convergence afforded by the natural orbitals ranges from approximately one step in  $N_{\text{max}}$  in the vicinity of the variational minimum ( $\hbar\omega \approx 15$ –20 MeV) to several steps in  $N_{\text{max}}$  towards the ends of the calculated  $\hbar\omega$  range.<sup>2</sup>

For the  ${}^6\text{He}$  proton radius, shown in Fig. 3(b), the natural orbital basis NCCI calculations lead the harmonic oscillator basis calculations in convergence by more than one step in  $N_{\text{max}}$  at  $\hbar\omega \approx 20$  MeV and by several steps in  $N_{\text{max}}$  at the high end of the  $\hbar\omega$  range. These radii obtained from the natural orbital calculations are also less dependent upon  $\hbar\omega$  than those obtained from the harmonic oscillator calculations.

The goal we set out to achieve is to find the true results for observables as they would be obtained in the full, infinite-dimensional space. Although full convergence is not achieved, even with the natural orbitals, the improved convergence motivates us to attempt to obtain estimates of the converged results via basis extrapolation methods [27, 29, 43, 44]. Infrared extrapolation schemes [27, 28, 45–47] are based on the premise that the solution of the many-body problem in a truncated space effectively imposes infrared (long-range) and ultraviolet (short-range) cutoffs. For bases with high enough  $\hbar\omega$  (and  $N_{\text{max}}$ ) ultraviolet convergence is assumed, and any remaining incomplete convergence is attributed to the failure of the basis to reproduce the long-range tail of the many-body wave function.

A basis consisting of harmonic oscillator orbitals with no more than  $N$  quanta cannot fully resolve long-range physics beyond the classical turning point  $L(N, \hbar\omega) = [2(N + 3/2)]^{1/2} b(\hbar\omega)$  [27],<sup>3</sup> where  $b(\hbar\omega) = (\hbar c)/[(m_N c^2)(\hbar\omega)]^{1/2}$  is again the oscillator length, with  $m_N$  the nucleon mass. The calculated energy and observables are expected to depend only on this cutoff  $L$ , approaching the true converged values as  $L \rightarrow \infty$ . For energy eigenvalues, it is expected that [45, 46]

$$E(L) = E_\infty + a_0 e^{-2k_\infty L}, \quad (1)$$

where  $E_\infty$ ,  $a_0$ , and  $k_\infty$  are to be deduced as fitting parameters from the results of calculations in truncated

<sup>2</sup> We consider steps of 2 in the number of oscillator quanta, since we restrict our attention to the positive parity sector for the present calculations.

<sup>3</sup> Specifically, we adopt the cutoff  $L_2(N, \hbar\omega) = [2(N + 2 + 3/2)]^{1/2} b(\hbar\omega)$  from Ref. [27] and take  $N = N_{\text{max}} + 1$ , since this is the highest number of oscillator quanta accessible to the neutrons in  ${}^6\text{He}$ . The single-particle space spanned by the natural orbitals is identical to that of the underlying harmonic oscillator orbitals, so the estimated length cutoff remains unchanged.

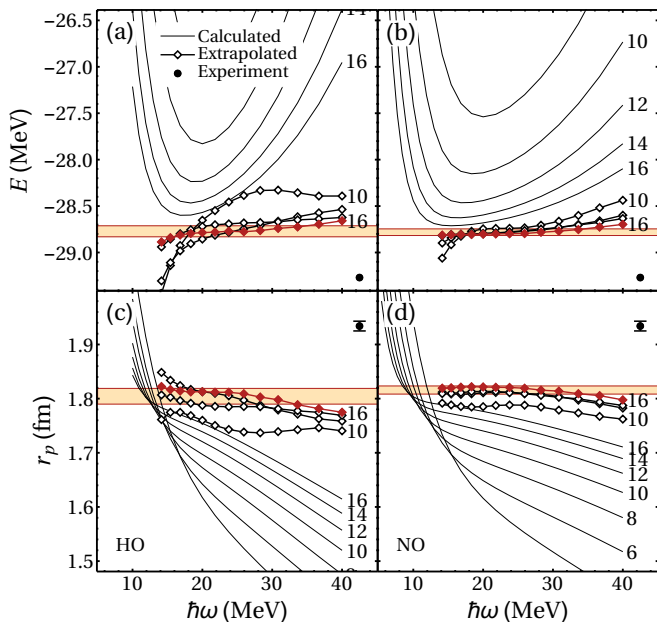


FIG. 4: Infrared basis extrapolations for the  ${}^6\text{He}$  ground state energy (top) and point proton radius (bottom), based on calculations in the harmonic oscillator basis (left) and natural orbital basis (right). The extrapolations (diamonds) are shown along with the underlying calculated results (plain lines) as functions of  $\hbar\omega$  at fixed  $N_{\text{max}}$  (as indicated). Experimental values (circles) are shown with uncertainties. The shaded bands reflect the mean values and standard deviations of the extrapolated results, at the highest  $N_{\text{max}}$ , over the  $\hbar\omega$  range considered.

spaces. Taking  $L \rightarrow \infty$ , we extract  $E_\infty$  as an estimate for the true energy. For mean square radii, it is expected that, letting  $\beta \equiv 2k_\infty L$ ,

$$r^2(L) = r_\infty^2 [1 - (c_0 + c_1 \beta^{-2}) \beta^3 e^{-\beta}], \quad (2)$$

for  $\beta \gg 1$ , where  $r_\infty$ ,  $c_0$ , and  $c_1$  are similarly deduced from calculations in truncated spaces, and  $r_\infty$  provides an estimate of the true RMS radius.

The extrapolated values for the  ${}^6\text{He}$  ground state energy and proton radius are shown in Fig. 4. We restrict ourselves to a straightforward application of (1) and (2), based on three-point extrapolation in  $N_{\text{max}}$  at fixed  $\hbar\omega$ . Calculations at low  $\hbar\omega$  may not provide the assumed ultraviolet convergence, while poor infrared convergence at high  $\hbar\omega$  leads to an excessively large correction and thus poor extrapolation.

The extrapolated  ${}^6\text{He}$  ground state energies from the natural orbital NCCI calculations [Fig. 4(b)] are considerably less  $\hbar\omega$ -dependent than the extrapolated energies from the harmonic oscillator NCCI calculations [Fig. 4(a)]. The extrapolations obtained for different  $N_{\text{max}}$  are also considerably more consistent (in the figure,  $N_{\text{max}}$  refers to the highest  $N_{\text{max}}$  in the three-point extrapolation). The extrapolated ground state energies obtained with the harmonic oscillator and natural orbital bases at  $\hbar\omega = 20$  MeV (chosen close to the variational energy minimum) and  $N_{\text{max}} = 16$  are consistent with

each other to within their respective variations, giving  $E \approx -28.79$  MeV and  $E \approx -28.80$  MeV, respectively.

Once the many-body calculation is under control, any remaining deviation of calculated values from nature may be attributed to deficiencies in the internucleon interaction. Comparing to the experimental binding energy of 29.27 MeV thus indicates that the JISP16 interaction underbinds  ${}^6\text{He}$  by  $\sim 0.5$  MeV.<sup>4</sup> (For comparison, the binding of  ${}^4\text{He}$  obtained with JISP16 matches experiment to within  $\sim 0.003$  MeV [29].)

The extrapolated proton radii extracted from the NCCI calculations with the natural orbital basis [Fig. 4(d)] similarly demonstrate a reduced  $\hbar\omega$  dependence and  $N_{\text{max}}$  dependence, as compared to the extrapolations from the oscillator-basis calculations [Fig. 4(c)]. At the highest calculated  $N_{\text{max}}$  ( $N_{\text{max}} = 16$ ), the extrapolated  $r_p$  varies only by  $\sim 0.02$  fm across the range of  $\hbar\omega$  values shown ( $\hbar\omega \approx 14$  MeV to 40 MeV), and the  $N_{\text{max}}$  dependence is comparable. We must emphasize that the variations in extrapolated values at best provide a rough guide to how well we can trust these extrapolated values as reflecting the true radius which would be obtained in an untruncated many-body calculation. Nonetheless, the  $\hbar\omega$ -independence and  $N_{\text{max}}$ -independence of the calculations at the  $\sim 0.02$  fm level is reassuring.

Taking the extrapolated proton radius at  $\hbar\omega = 20$  MeV and  $N_{\text{max}} = 16$  as representative gives  $r_p \approx 1.82$  fm.<sup>5</sup> Thus, it would appear that the *ab initio* NCCI calculations with the JISP16 interaction, while qualitatively reproducing the increase in proton radius with the onset of halo structure in  ${}^6\text{He}$ , do yield a quantitative shortfall of  $\sim 0.12$  fm (or  $\sim 6\%$ ) for the proton radius of  ${}^6\text{He}$ .

#### IV. CONCLUSION

Describing the nuclear many-body wave function within truncated spaces is challenging due to the need to describe, simultaneously, long-range asymptotics and short-range correlations. Natural orbitals, obtained here by diagonalizing one-body density matrices from initial NCCI calculations using the harmonic oscillator basis, build in contributions from high-lying oscillator shells, thereby accelerating convergence.

In the present application to the halo nucleus  ${}^6\text{He}$ , improvement is by about one step in  $N_{\text{max}}$  near the variational minimum in  $\hbar\omega$ , and significantly more for other  $\hbar\omega$  values (Fig. 3). To put these gains in perspective, we note that an increment in  $N_{\text{max}}$  results in an increase

<sup>4</sup> The present extrapolations for the  ${}^6\text{He}$  ground state energy are consistent with the estimate  $E = -28.8(1)$  MeV [30] obtained from the *ad hoc* exponential basis extrapolation scheme for the oscillator basis [29, 43].

<sup>5</sup> The present extrapolated result for the  ${}^6\text{He}$  proton radius is consistent with previous estimates [35] based on the “crossover point” [43] of successive  $N_{\text{max}}$  curves in a plot such as Fig. 3(b).

in matrix dimension of about a factor of 3-5, as seen in Fig. 1, with much larger increase in the computational costs [48]. Although full convergence is still not achieved, the calculations using natural orbitals provide improved basis parameter independence for extrapolations with respect to the infrared cutoff of the basis (Fig. 4).

The successful application of natural orbitals to *ab initio* nuclear NCCI calculations presented here provides a starting point for exploring ideas (some taken from electron structure theory) which may more fully realize the potential of the natural orbital approach:

(1) NCCI calculations based on natural orbitals yield improved one-body densities which can, in turn, be diagonalized to yield new natural orbitals. Natural orbitals constructed through such an iterative method can rapidly build in additional contributions from high-lying shells, thereby potentially further accelerating convergence [20, 49].

(2) An improved reference basis for the initial NCCI calculation may also boost the convergence of the subsequent natural orbital calculations. For instance, the Laguerre functions, commonly used as the starting point for natural orbitals in electron-structure calculations, also have the correct exponential asymptotics for nucleons bound by a finite-range potential.

(3) The structure of nuclear excited states can vary markedly from that of the ground state. Natural orbitals constructed by diagonalizing the density matrices from excited states, rather than from the ground state, may

more effectively accelerate convergence of those excited states [20].

(4) Finally, natural orbitals are conducive to a more efficient many-body truncation scheme than the conventional oscillator  $N_{\max}$  scheme. The eigenvalues associated with the natural orbitals, by providing an estimate of the mean occupation of each orbital in the many-body wave function, also suggest a means of estimating the relative importance of Slater determinants involving these orbitals.

### Acknowledgements

We thank G. Hupin for valuable discussions on the formulation of the nuclear natural orbital problem and M. A. McNanna for carrying out informative preliminary studies in one dimension. This material is based upon work supported by the U.S. Department of Energy, Office of Science, under Award Numbers DE-FG02-95ER-40934, DESC0008485 (SciDAC/NUCLEI), and DE-FG02-87ER40371. This research used computational resources of the University of Notre Dame Center for Research Computing and of the National Energy Research Scientific Computing Center (NERSC), a U.S. Department of Energy, Office of Science, user facility supported under Contract DE-AC02-05CH11231.

- 
- [1] S. C. Pieper, R. B. Wiringa, and J. Carlson, Phys. Rev. C **70**, 054325 (2004).
- [2] T. Neff and H. Feldmeier, Nucl. Phys. A **738**, 357 (2004).
- [3] G. Hagen, D. J. Dean, M. Hjorth-Jensen, T. Papenbrock, and A. Schwenk, Phys. Rev. C **76**, 044305 (2007).
- [4] S. Quaglioni and P. Navrátil, Phys. Rev. C **79**, 044606 (2009).
- [5] S. Bacca, N. Barnea, and A. Schwenk, Phys. Rev. C **86**, 034321 (2012).
- [6] N. Shimizu, T. Abe, Y. Tsunoda, Y. Utsuno, T. Yoshida, T. Mizusaki, M. Honma, and T. Otsuka, Prog. Exp. Theor. Phys. **2012**, 01A205 (2012).
- [7] T. Dytrych, K. D. Launey, J. P. Draayer, P. Maris, J. P. Vary, E. Saule, U. Catalyurek, M. Sosonkina, D. Langr, and M. A. Caprio, Phys. Rev. Lett. **111**, 252501 (2013).
- [8] B. R. Barrett, P. Navrátil, and J. P. Vary, Prog. Part. Nucl. Phys. **69**, 131 (2013).
- [9] S. Baroni, P. Navrátil, and S. Quaglioni, Phys. Rev. C **87**, 034326 (2013).
- [10] R. B. Wiringa, V. G. J. Stoks, and R. Schiavilla, Phys. Rev. C **51**, 38 (1995).
- [11] D. R. Entem and R. Machleidt, Phys. Rev. C **68**, 041001 (2003).
- [12] A. M. Shirokov, J. P. Vary, A. I. Mazur, and T. A. Weber, Phys. Lett. B **644**, 33 (2007).
- [13] E. Epelbaum, H.-W. Hammer, and U.-G. Meißner, Rev. Mod. Phys. **81**, 1773 (2009).
- [14] M. Freer, Rep. Prog. Phys. **70**, 2007 (2149).
- [15] B. Jonson, Phys. Rep. **389**, 1 (2004).
- [16] I. Tanihata, H. Savajols, and R. Kanungo, Prog. Part. Nucl. Phys. **68**, 215 (2013).
- [17] P.-O. Löwdin, Phys. Rev. **97**, 1474 (1955).
- [18] H. Shull and P.-O. Löwdin, J. Chem. Phys. **23**, 1565 (1955).
- [19] P.-O. Löwdin and H. Shull, Phys. Rev. **101**, 1730 (1956).
- [20] E. R. Davidson, Rev. Mod. Phys. **44**, 451 (1972).
- [21] C. Mahaux and R. Sartor, Adv. Nucl. Phys. **20**, 1 (1991).
- [22] M. V. Stoitsov, A. N. Antonov, and S. S. Dimitrova, Phys. Rev. C **48**, 74 (1993).
- [23] T. Helgaker, P. Jørgensen, and J. Olsen, *Molecular Electron-Structure Theory* (Wiley, Chichester, 2000).
- [24] A. E. McCoy and M. A. Caprio, J. Math. Phys. **57**, 021708 (2016).
- [25] M. Moshinsky and Y. F. Smirnov, *The Harmonic Oscillator in Modern Physics* (Harwood Academic Publishers, Amsterdam, 1996).
- [26] J. Suhonen, *From Nucleons to Nucleus* (Springer-Verlag, Berlin, 2007).
- [27] R. J. Furnstahl, G. Hagen, and T. Papenbrock, Phys. Rev. C **86**, 031301 (2012).
- [28] S. N. More, A. Ekstrom, R. J. Furnstahl, G. Hagen, and T. Papenbrock, Phys. Rev. C **87**, 044326 (2013).
- [29] P. Maris, J. P. Vary, and A. M. Shirokov, Phys. Rev. C **79**, 014308 (2009).
- [30] P. Maris and J. P. Vary, Int. J. Mod. Phys. E **22**, 1330016 (2013).

- [31] M. A. Caprio, P. Maris, J. P. Vary, and R. Smith, *Int. J. Mod. Phys. E* **24**, 1541002 (2015).
- [32] L. Schäfer and H. A. Weidenmüller, *Nucl. Phys. A* **174**, 1 (1971).
- [33] M. A. Caprio, P. Maris, and J. P. Vary, *Phys. Rev. C* **86**, 034312 (2012).
- [34] G. Hagen, M. Hjorth-Jensen, and N. Michel, *Phys. Rev. C* **73**, 064307 (2006).
- [35] M. A. Caprio, P. Maris, and J. P. Vary, *Phys. Rev. C* **90**, 034305 (2014).
- [36] D. R. Tilley, C. M. Cheves, J. L. Godwin, G. M. Hale, H. M. Hofmann, J. H. Kelley, C. G. Sheu, and H. R. Weller, *Nucl. Phys. A* **708**, 3 (2002).
- [37] J. L. Friar, J. Martorell, and D. W. L. Sprung, *Phys. Rev. A* **56**, 4579 (1997).
- [38] L.-B. Wang, P. Mueller, K. Bailey, G. W. F. Drake, J. P. Greene, D. Henderson, R. J. Holt, R. V. F. Janssens, C. L. Jiang, Z.-T. Lu, T. P. O'Connor, R. C. Pardo, K. E. Rehm, J. P. Schiffer, and X. D. Tang, *Phys. Rev. Lett.* **93**, 142501 (2004).
- [39] M. Brodeur, T. Brunner, C. Champagne, S. Ettenauer, M. J. Smith, A. Lapierre, R. Ringle, V. L. Ryjkov, S. Bacca, P. Delheij, G. W. F. Drake, D. Lunney, A. Schwenk, and J. Dilling, *Phys. Rev. Lett.* **108**, 052504 (2012).
- [40] Z.-T. Lu, P. Mueller, G. W. F. Drake, W. Nörtershäuser, S. C. Pieper, and Z.-C. Yan, *Rev. Mod. Phys.* **85**, 1383 (2013).
- [41] P. Maris, M. Sosonkina, J. P. Vary, E. Ng, and C. Yang, *Procedia Comput. Sci.* **1**, 97 (2010).
- [42] H. M. Aktulga, C. Yang, E. G. Ng, P. Maris, and J. P. Vary, *Concurrency Computat.: Pract. Exper.* **26**, 2631 (2013).
- [43] S. K. Bogner, R. J. Furnstahl, P. Maris, R. J. Perry, A. Schwenk, and J. Vary, *Nucl. Phys. A* **801**, 21 (2008).
- [44] S. A. Coon, M. I. Avetian, M. K. G. Kruse, U. van Kolck, P. Maris, and J. P. Vary, *Phys. Rev. C* **86**, 054002 (2012).
- [45] R. J. Furnstahl, S. N. More, and T. Papenbrock, *Phys. Rev. C* **89**, 044301 (2014).
- [46] R. J. Furnstahl, G. Hagen, T. Papenbrock, and K. A. Wendt, *J. Phys. G* **42**, 034032 (2015).
- [47] K. A. Wendt, C. Forssén, T. Papenbrock, and D. Sääf, *Phys. Rev. C* **91**, 061301 (2015).
- [48] J. P. Vary, P. Maris, E. Ng, C. Yang, and M. Sosonkina, *J. Phys. Conf. Ser.* **180**, 012083 (2009).
- [49] C. F. Bender and E. R. Davidson, *J. Phys. Chem.* **70**, 2675 (1966).